This is a bit futuristic

Near-infrared finger vein patterns for personal identification

Miyuki Kono, Hironori Ueki, and Shin-ichiro Umemura

We have demonstrated a personal identification system that is based on near-infrared finger vein patterns. Finger vein patterns of 678 volunteers are acquired by transmitting near-infrared light through a finger and capturing the image with a CCD camera. These vein patterns are enhanced by a background-reduction filter. The similarity between two patterns is then quantified by use of the normalized maximum of the cross correlation of the two images after correction of the tilt angle. The enhanced finger vein pattern enabled 678 persons to be successfully identified.

OCIS codes: 170.0170, 170.3880, 100.5010.

1. Introduction

Electronically accessible accurate personal identification is becoming more and more necessary. On-line personal identification has already been used to access control of financial transactions including electronic commerce. ID cards, and passwords have been used in these applications, but they can be easily stolen or forgotten. To ensure higher security, several ways of biometrics-based identification have started being used. One of the well-known biometrics technologies is fingerprint recognition.[1–4] Iris scanning, retina scanning, voice verification, and face recognition have also been used.[5–11] But each biometrics technology has some problems. Fingerprint identification requires physical contact, iris and retina scanning produces an unpleasant feeling due to shining a strong light into the subject's eyes, and voice verification and face recognition are not as accurate as fingerprint recognition.[12–15] If a method employing biometrics technology, accurate and free from contagion and unpleasant feelings, is available, it can be adopted in general public use, such as for ATMs (Automatic Teller Machines) and new applications, such as for patient identification in hospitals.

In the present study, we investigated the potentiality of near-infrared finger vein patterns for personal identification. We developed an experimental prototype using near-infrared light transmitted through the finger. Light transmission through tissues is greatest within the red and near-infrared wavelength bands.[16–18] At visible wavelengths, transmission diminishes because of electronic absorption in tissue pigments, such as hemoglobin, myoglobin, and melanins. At longer infrared wavelengths, broad and intense absorption bands correspond to the fundamental vibration modes of water bonds. At near-infrared wavelengths, hemoglobin has lower absorbance than at visible wavelengths, but it is relatively high compared to other proteins in the tissue. Therefore transmitting near-infrared light through a finger is suitable for acquisition of its vein pattern. The possibility of obtaining a personal identification based on the vein pattern acquired by transmitting light through a hand was indicated a decade ago,[19] but it has not been demonstrated. Personal identification using near-infrared finger vein patterns was first demonstrated with our prototype.[20] Further study has been made to quantify the information in the finger vein pattern essential for personal identification and is reported in this paper.

2. Materials and Methods

Experimental prototype. Figs. 1 and 2 show a block diagram of the prototype for the experiment and the optical configuration, respectively. An array of mold type near-infrared LEDs (L810-06AU, Epitex) was used as a light source (wavelength: 810 nm). Both sides of a plastic lens attached to an LED were made flat to increase the number of LEDs per

The authors are with Medical Systems Research Department, Central Research Laboratory, Hitachi Limited, 1-280 Higashi-koigakubo Kokubunji-shi, Tokyo 185-8601, Japan.

Received 12 April 2002; revised manuscript received 15 August 2002.

0003-6935/02/357429-08$15.00/0

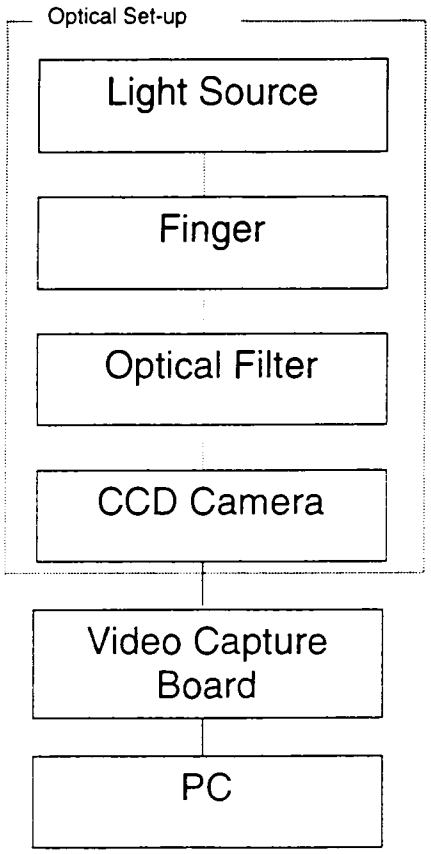

Fig. 1. Block diagram of the prototype for the experiment.

length in the array. The dorsal side of the finger was illuminated with the LED array, and the transmitted light through the finger was received by an infrared-sensitive CCD camera (NC300AIR, Takenaka System) with a neutral-density filter. The palm side of the finger vein pattern was thereby acquired [see Fig. 3(a)], and the image data were sent to a PC (Dimension XPS-T750r, Dell Computer) via a video-capture board (METEOR2-MC/4, Matrox). A

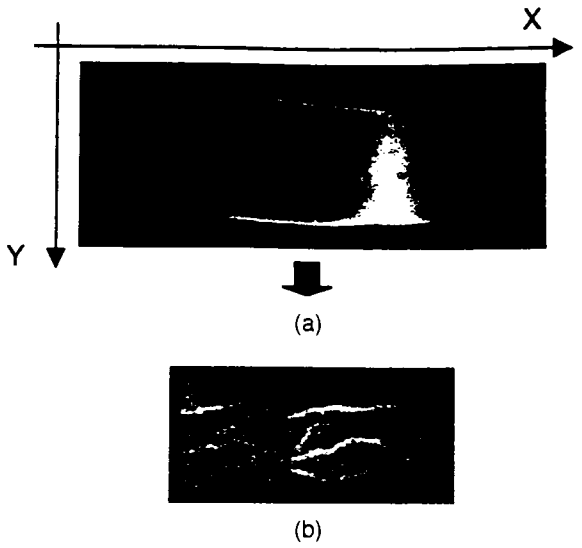

Fig. 3. Examples of an image of a finger vein pattern: (a) captured image by CCD camera, (b) enhanced vein-pattern image.

640 × 480 pixel gray-scale still image of the finger was captured and processed. The current level of the LEDs was manually adjusted when the intensity of the light transmitted through the finger was too high or too low. The angle of the palm to the vertical was maintained at less than several degrees when the image was captured.

Scheme of image processing. Fig. 3 shows an example of an image of a finger vein pattern captured with the CCD camera (a) and the image of its enhanced vein pattern (b). The steps of the image processing are described next (see Fig. 4). At first, low-pass filter A was used to reduce the background noises and detect the shape of the finger. The low-pass filter replaces a pixel's value with the average of its original value and those of its eight surrounding neighbors. Directional differentiation in the y direction was performed to obtain the image of the edge of

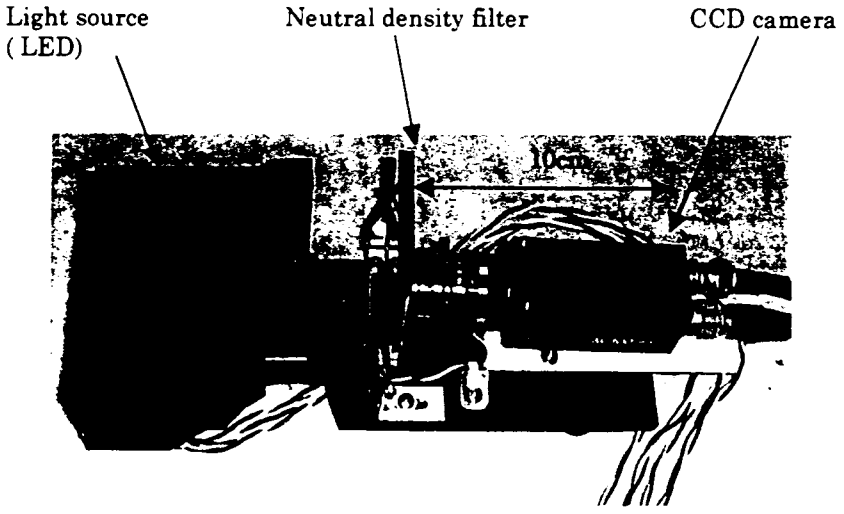

Fig. 2. Optical configuration.

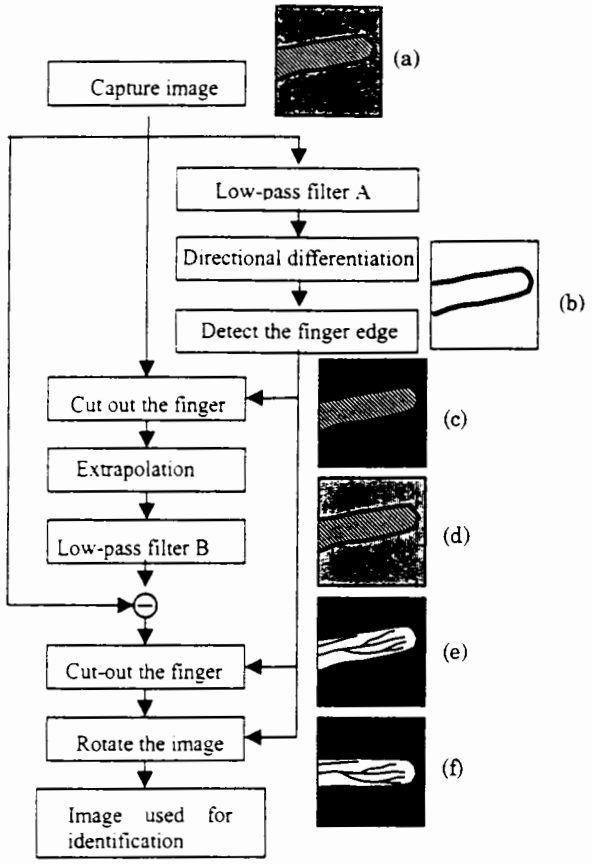

Fig. 4. Steps in image processing.

the finger [Fig. 4, third step of (b)]. The edge of the finger has a relatively higher image intensity, so the image inside it was easily cut out, and its outside was zero padded (c), and its intensity was assigned to the pixels in its periphery. Then, the image was put through the low-pass filter B so that the background profile (d) was obtained. Here, the low-pass filter replaces the intensity of a pixel with the average of its original intensity and those of the predetermined number of its surrounding neighbors. An image of an enhanced finger vein pattern was obtained by subtracting the background profile (d) from the captured image (a). We used an $M \times M$ pixel array for the low-pass filtering, and the number of M was chosen so as to optimize the enhancement for the best performance of personal identification. Last, the tilt angle of the finger from the horizon (e) was calculated using the image of the finger edge (b), and the angle was corrected to zero (f). Then, the obtained image was registered. The similarity between two registered images was evaluated based on the correlation coefficient between them. Let p and q be $N \times N$ square matrices of image data, then the correlation between them is defined as

$$y_{i,j} = \mathrm{IFFT2}[{}^{*}\mathrm{FFT2}(p) \circ \mathrm{FFT2}(q)],$$
$$i, j = 1, 2, \ldots N, \tag{1}$$

where FFT2 denotes two-dimensional fast Fourier transform (FFT), IFFT2 denotes two-dimensional inverse FFT, * denotes complex conjugate, and ○ denotes element-by-element multiplication.

It was normalized as

$$Y_{i,j} = y_{i,j} \left[\sum_{k=1}^{N} \sum_{l=1}^{N} P_{k,l}(u)^2 \cdot \sum_{k=1}^{N} \sum_{l=1}^{N} Q_{k,l}(u)^2 \right]^{1/2},$$
$$i, j, k, l = 1, 2, \ldots, N, \tag{2}$$

where $P_{k,l}(u) = {}^{*}\mathrm{FFT2}(p)$, $Q_{k,l}(u) = \mathrm{FFT2}(q)$.

The normalized cross correlation between the two images was defined as

$$C = [\max(Y_{i,j})]^{1/2}. \tag{3}$$

The size of an image captured by the CCD camera was 640 × 480 pixels. At first, an image with 512 × 480 pixels was cut out from it, and zero padding made an image with 512 × 512 pixels. To determine the minimum quantity of image information necessary for identifying one person from the others in the sampled group, the effect of step-by-step reduction in image data size was tested. Here, the sum of the intensity of the nearest four pixels was used as the intensity of the corresponding pixel in the reduced image, which was also reduced in the same way at the next step. The image data size was thereby reduced by factors of two in the x and y directions.

Sampled group. Finger vein patterns of 678 volunteers were acquired during a yearly medical checkup of the employees at the Central Research Laboratory in May and June of 2000. Most of the volunteers were in their 20s and 30s (479 males and 199 females). In this paper, we report the result of personal identification using the vein patterns of their left little fingers. Two images were captured per each volunteer, one was registered as the reference image, and the other was used as an image to be tested.

Valuation of identification accuracy. A normalized false acceptance rate (FAR) and a normalized false rejection rate (FRR) are defined as

$$\mathrm{FAR}(T) = [N(r_d > T)]/N_2. \tag{4}$$

$$\mathrm{FRR}(T) = [N(r_s \le T)]/N_1, \tag{5}$$

where T is the threshold, N_1 is the number of samples (678), and N_2 is the number of combinations of 678 images, i.e., 229,503. And r_d and r_s are the correlation coefficient between two patterns from different individuals and from the same individual, respectively.

To evaluate the identification accuracy of the proposed method, we define total error rate (TER) as the following:

$$\mathrm{TER} = \left\{ \int_0^1 [\mathrm{FAR}(T) \times \mathrm{FRR}(T)]\mathrm{d}T \right\}^{1/2}. \tag{6}$$

TER ranges from zero to one. When 678 images are identified completely, i.e., FAR (T) and FRR (T) form no crossing area, TER is zero.

Prediction of accuracy for larger groups. The ac-

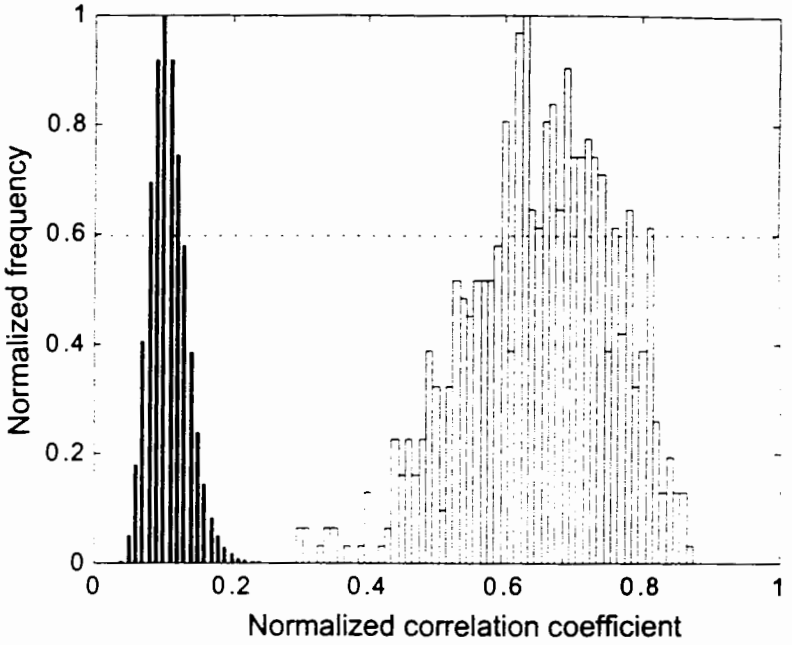

Fig. 5. Histograms of the normalized correlation coefficient between two images of the 678 individuals. White bars denote the results from the two images of each individual, black bars denote the results from two different individuals.

curacy of the proposed method of personal identification in the case when it is applied to larger groups was predicted based on the results from 678 individuals. Both FAR and FRR plots against T were curve fitted by a least-squares method in the range of T, where both rates are close to zero. Then, rates on each fitted curve were used to predict the false rate as a function of the threshold for larger groups.

The Kolmogorov–Smirnov test[21–23] was applied to test goodness-of-fit. In this test, the determined critical value, $D_{\alpha,n}$, when the level of significance and the sample size equals α and n, respectively, was used.

$$G = \max |F(T) - S(T)| - D_{\alpha,n}, \tag{7}$$

where $F(T)$ denotes fitted distribution function and $S(T)$ denotes data from the sample. If G is greater than zero, then the hypothesis that the censored sample comes from the fully specified continuous distribution $F(T)$ is rejected at the chosen level of confidence. To test the validity of using curve-fitted data as the predicted false rates for larger groups, false rates obtained from the results from 678 individuals were substituted for $S(T)$, and those on the fitted curves were for $F(T)$.

3. Results and Discussion

Figure 5 shows the histograms of a normalized correlation coefficient between two images from the 678 individuals. White bars denote the results from each individual, and black bars denote the results from two different individuals. All 678 individuals were perfectly identified. Here, the image matrix size was 512 × 512 pixels and M was 25. This result clearly demonstrates the efficacy of personal identification based on near-infrared finger vein patterns.

The effect of the matrix size for low-pass filtering, M, was also examined, and the results are shown in Figs. 6, 7, and 8. The x axis denotes a threshold, T, and the y axis denotes the FAR and FRR corresponding to the threshold. In Fig. 6, FAR and FRR curves shift to the left-hand side as M increases up to 25, and they shift to the right-hand side as M increases above 25. Figures 7 and 8 are FAR versus FRR plots. The area around the origin in Fig. 7 is enlarged and plotted in Fig. 8. When M is 25, 40, 50, 64, and 75, the plotted points are located close to the origin, i.e., high accuracy of identification can be achieved. This is summarized by the TER plotted against M (filled circles) in Fig. 9. Here, TERs for a nonsquare low-pass filter B are also plotted. The filled triangles and squares denote the TER for a low-pass filter B of 50 × 25 and 25 × 50 pixels, respectively. In this comparison, square filters showed much better accuracy of identification than nonsquare filters. For simplicity of signal processing, M = 25, the smallest size of filter B that gave zero TER at a certain threshold, was chosen.

To investigate the minimum data size required to identify 678 persons perfectly, FAR and FRR for various sizes of image data were calculated and plotted in Fig. 10. Here, it is shown that FAR and FRR can be zero simultaneously at a certain threshold when the image size is not less than 32 × 32. This is summarized by TER plotted against the image size in the x direction in Fig. 11. Here, TERs for the image aspect ratio of 1:4 were also plotted in addition to those of 1:1. For the aspect ratio of 1:4, the minimum image data size required for perfect identification of 678 individuals lies at approximately 16 × 64

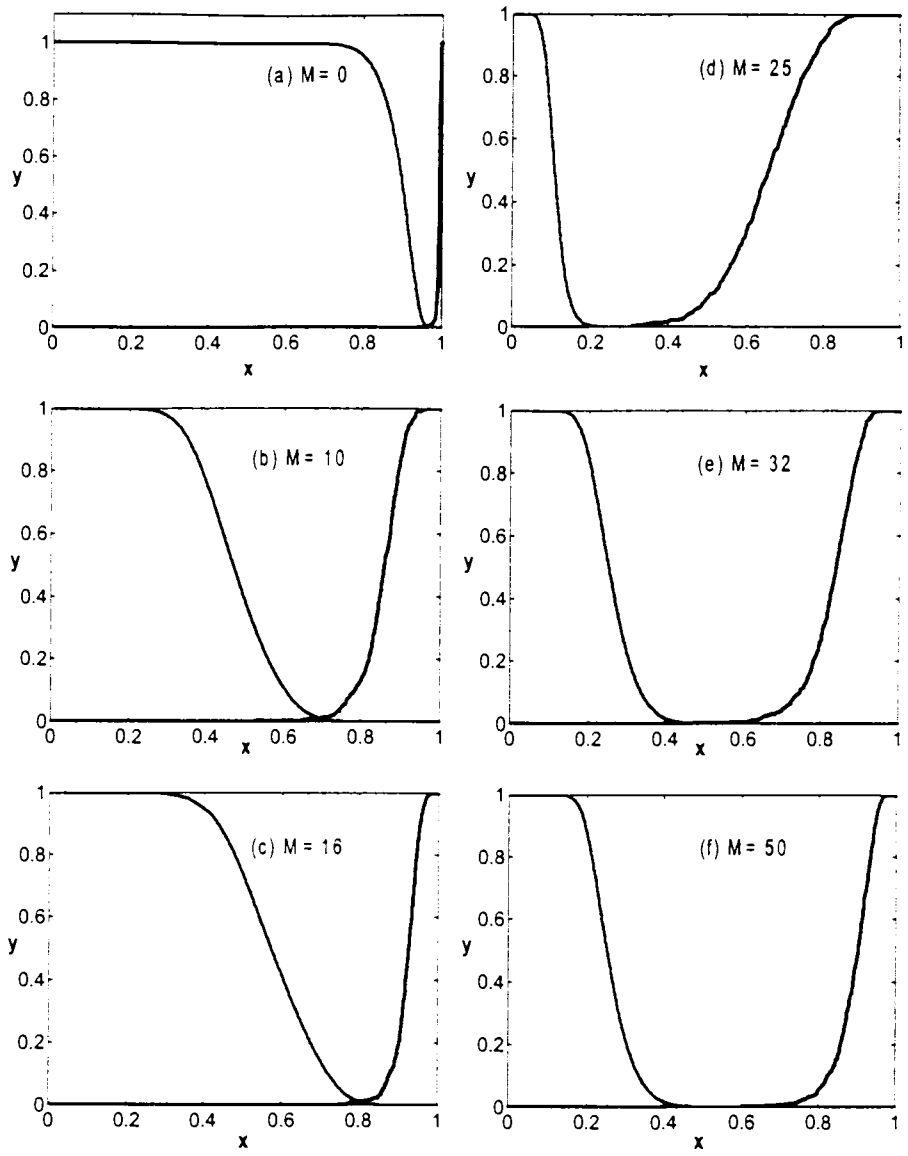

Fig. 6. Effect of the matrix size for low-pass filtering, M. Black curves denote FRRs, gray curves denote FARs.

pixels. Both results show that the perfect identification requires an image size of approximately 10^3 pixels.

Table 1 and Table 2 list the changes in TER according to the reduction of image size in only the x and y direction, respectively. When the image data size in the x direction was kept to 128 pixels and the size in the y direction was changed, the minimum data size in the y direction for perfect identification of the 678 persons was 16. When the image data size in the y direction was kept to 128 pixels, the minimum data size in the x direction was 8 pixels. In this comparison, a larger image size was required, i.e., less image reduction was allowed, in y direction than in the x direction. This may be reasonable considering that finger vein patterns run from the finger root to the tip in the x direction.

Monoexponential curves are fitted to FAR and FRR as functions of T by a least-squares method in the

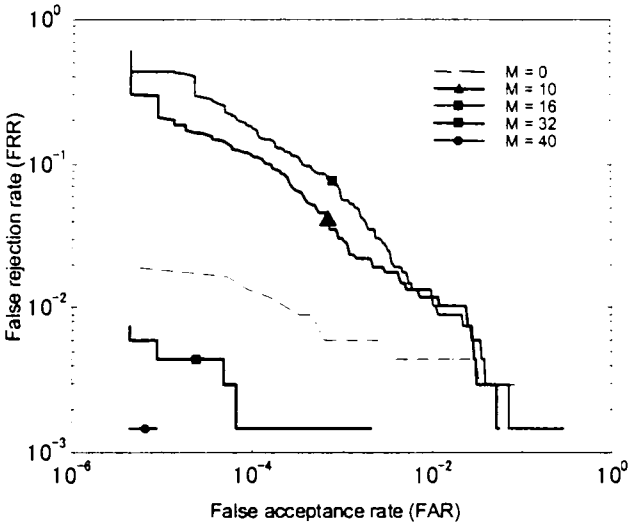

Fig. 7. FAR vs. FRR.

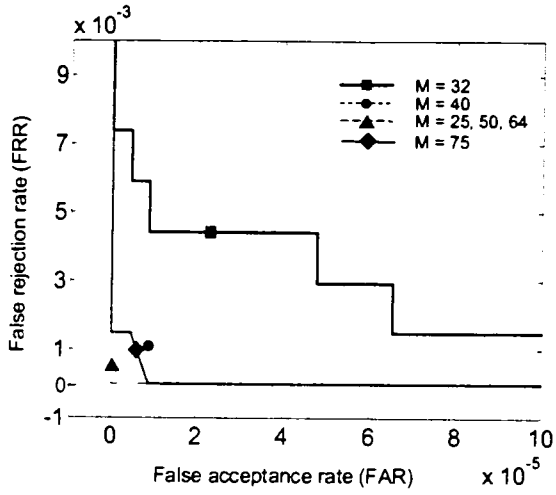

Fig. 8. FAR vs. FRR around the origin.

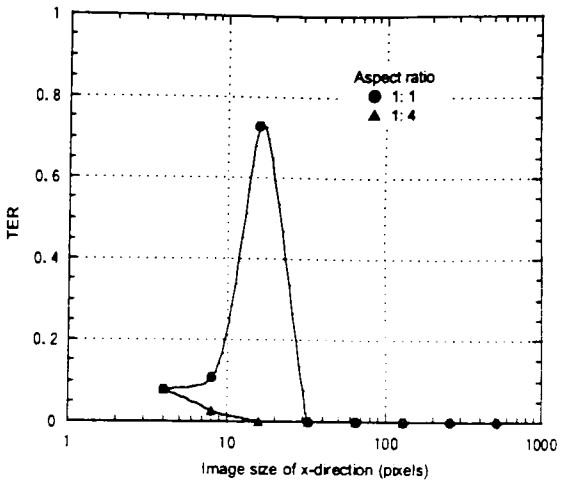

Fig. 11. TER plots of an image with aspect ratio of 1:1 and 1:4.

range of T, where each false rate is less than a certain level. In Fig. 12, the curve fitting to the false rates less than 0.15 is shown for image sizes of 512 × 512, 128 × 128, and 32 × 32 pixels. The goodness-of-fit was confirmed by the Kolmogorov-Smirnov test. Table 3 lists $D_{\max} = \max|F(T) - S(T)|$ and the critical values, $D_{0.01}$, for a level of significance of 0.01 for image sizes from 512 × 512 to 32 × 32 pixels for both FAR and FRR plots. Because $D_{\max}$ is less than $D_{0.01}$, i.e. $G = D_{\max} - D_{0.01}$ is negative, for every case, the goodness of all fitted curves was confirmed at a level of significance of 0.01.

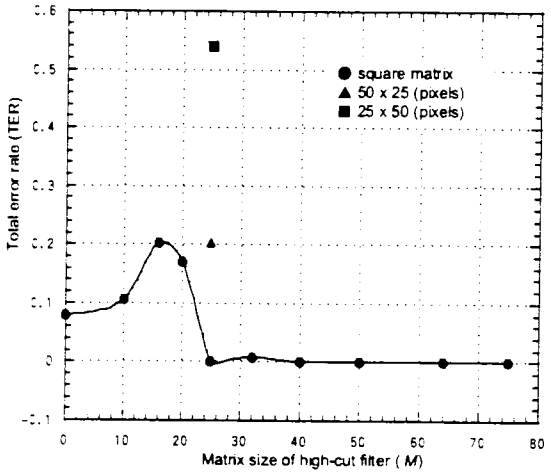

Fig. 9. Change of TER according to the change of M.

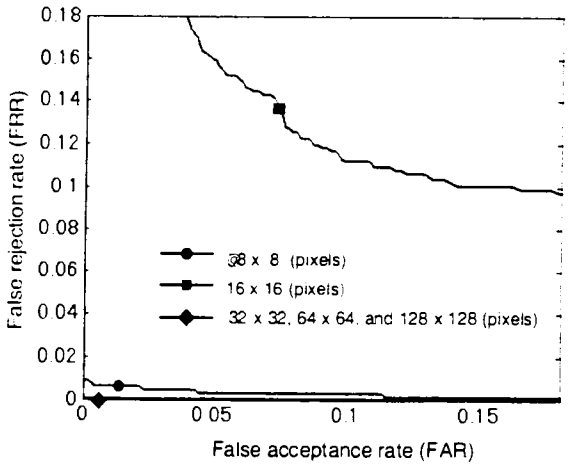

Fig. 10. FAR vs. FRR with various image sizes.

The relation between FAR and FRR for larger groups can be predicted from the fitted curves. The predicted FARs corresponding to an FRR of 0.1% are shown in Fig. 13. The lowest predicted FAR was merely $3.5 \times 10^{-5}\%$ at an image size of 128 × 128 pixels. The image size reduction by use of a summation of the nearest four pixels reduces the pixel noise, and this may be effective to reduce the FAR until the image size is reduced to 128 × 128 pixels. However, further image reduction may result in too much loss of information and the increment of the FAR. If an FAR of 0.043% is allowed, the image size used for identification can be reduced to 32 × 32 pixels. These results suggest that near-infrared finger vein patterns may show an accuracy of personal identification equivalent to or higher than irises and fingerprints[4,15] when applied to larger groups. However, we must admit that the genetic and age variations in the tested 678 persons are much smaller than

Table 1. Change of TER according to the change of aspect ratio of an image

X × Y (pixels)	8 × 128	16 × 128	32 × 128	64 × 128	128 × 128
TER	4.2×10^{-4}	0	0	0	0

Table 2. Change of TER according to the change of aspect ratio of an image

X × Y (pixels)	128 × 8	128 × 16	128 × 32	128 × 64	128 × 128
TER	2.8×10^{-1}	1.5×10^{-2}	1.6×10^{-4}	0	0

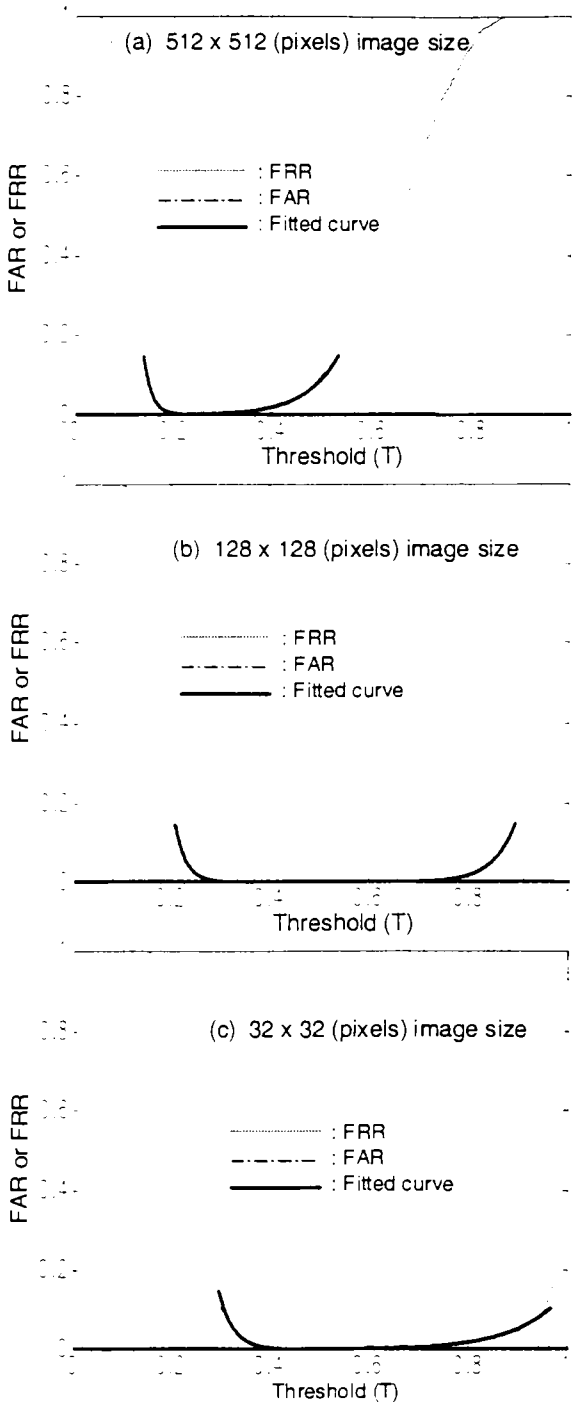

Fig. 12. Curve fitting of FAR and FRR.

in the entire human population. Further study is needed to test its accuracy in a large group with a large genetic and age variation.

The near-infrared image of a finger vein pattern has several different kinds of background noises. Light transmits relatively easily through the joints of the finger. This creates low spatial frequency background noises in the image of finger veins. Linear two-dimensional filtration was used to remove these kinds of noises in this paper. We also tried median

Table 3. Kolmogorov-Smirnov test on goodness-of-fit[a]

Image sizes (pixels)	FRR plot			FAR plot		
	D_{max}	$D_{0.01}$	n	D_{max}	$D_{0.01}$	n
512 × 512	0.0304	0.1646	98	0.0081	0.0090	32604
128 × 128	0.0342	0.1629	100	0.0085	0.0090	32506
32 × 32	0.0565	0.1654	97	0.0032	0.0090	32696

[a]on the FAR and FRR curves.

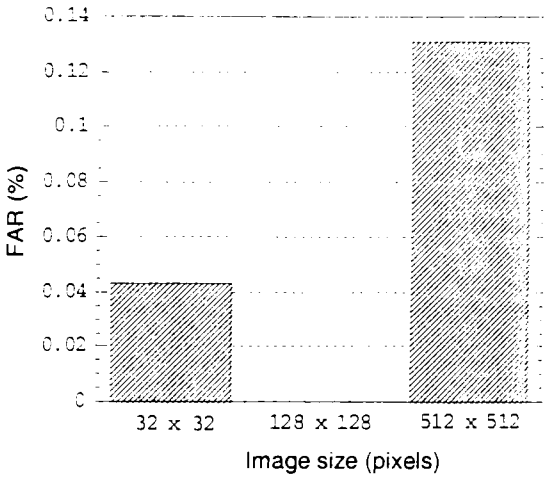

Fig. 13. Predictive FAR values with larger groups when the permitted FRR is 0.1 percent.

filters, but found them inadequate. Ridge extraction and thinning of ridges,[1,2] which are often used for fingerprint recognition, were tried but they were also found unsuitable for vein-pattern matching. However, there may be some other signal-processing techniques and filters, such as a nonlinear filter that may show better performances than the filters proposed in this paper in extracting and enhancing the patterns.

Conclusions

We have demonstrated that accurate personal identification is possible by using near-infrared finger vein patterns. A near-infrared transmission image of a finger was captured, and its vein pattern was enhanced by a background reduction two-dimensional linear filter. By optimizing the filter parameters, all 678 members of the sampled group were perfectly identified. Perfect identification was achieved until the image data size was reduced up to approximately 10^3 pixels. Curve fitting to an FAR and an FRR, plotted against a threshold, made a prediction for larger groups possible. When the FRR is fixed to 0.1%, the predicted FAR was merely 3.5×10^{-5}% at an image size of 128 × 128 pixels and 0.043% at an image size of 32 × 32 pixels. This level of accuracy is equivalent to or higher than that of irises and fingerprints.

The most important remaining problem for the personal identification based on near-infrared finger vein patterns may be the possible change in the vein pattern in a lifetime. This must be studied although

it may take a long period of tracking time. The study period could be shortened by tracking children's rather than adults' finger vein patterns.

This research has been performed under the sponsorship of Hitachi Ltd., Hitachi Credit Corporation (renamed as Hitachi Capital Corporation), and Hitachi Software Engineering. The authors thank the 678 volunteers for their help in our experiment. We are also thankful to Hitachi Computer Peripherals for the technical support.

References

1. M. Trauring, "Automatic comparison of finger-ridge patterns," Nature **197,** 938–940 (1963).
2. A. Jain, L. Hong, S. Pankanti, and R. Bolle, "An identity authentication system using fingerprints," Proc. IEEE **85,** 1365–1388 (1997).
3. M. Tico, P. Kuosmanen, and J. Saarinen, "Wavelet domain features for fingerprint recognition," Electron. Lett. **37,** 21–22 (2001).
4. Ultra-Scan Corporation, "Benchmark test comparing fingerprint imaging technology," http://www.ultra-scan.com new.htm.
5. J. Ashbourn, *Biometrics: Advanced Identity Verification* (Springer, London, 2000).
6. J. G. Daugman, "High confidence visual recognition of persons by a test of statistical independence," IEEE Trans. Pattern Anal. Mach. Intell. **15,** 1148–1161 (1993).
7. Y. Zhu, T. Tan, and Y. Wang, "Biometric personal identification based on iris patterns," in *Proceedings of the 15th International Conference on Pattern Recognition*, (Barcelona, Spain, 2000), pp. 805–808.
8. T. Kohonen, *Self-Organization and Associative Memory*, (Springer-Verlag, Berlin, 1988).
9. M. A. Turk and A. P. Pentland, "Face recognition using eigenfaces," Proc. IEEE Conference on Computer Vision and Pattern Recognition, 586–591 (1991).
10. A. Martin and M. Przybocki, "The NIST 1999 speaker recognition evaluation: an overview," http: www.nist.gov speech publications papersrc spk99oview.pdf.
11. M. Kawasaki, "The performance of retinal scan," Electronics **550,** 24–26 (2000), (in Japanese).
12. S. Liu and M. Silverman, "A practical guide to biometric security technology," IT Professional **3,** 27–32 (2001).
13. Communications-Electronics Security Group, "Best practices in testing and reporting performance of biometric devices," http://www.cesg.gov.uk/technology/biometrics/media/Best%20Practice.pdf.
14. S. Pankanti, R. M. Bolle, and A. Jain, "Biometrics: The future of identification," Computer **33,** 46–49 (2000).
15. Centre for Mathematics and Scientific Computing National Physical Laboratory, "Biometric product testing final report," http://www.cesg.gov.uk/technology/biometrics/media/Biometric%20Test%20Report%20pt1.pdf.
16. J. D. Hardy, H. T. Hammel, and D. Murgatroyd, "Spectral transmittance and reflectance of excised human skin," J. Appl. Phys. **9,** 257–264 (1956).
17. B. C. Wilson, M. S. Patterson, S. T. Flock, and J. D. Moulton, "The optical absorption and scattering properties of tissues in the visible and near-infrared wavelength range," in *Light in Biology and Medicine; Vol. 1*, R. H. Douglas, J. Moan, and F. D. Acqua, eds. (Plenum, New York, 1988), pp. 45–52.
18. H. Key, P. C. Jackson, and P. N. T. Wells, "New approaches to transillumination imaging," J. Biomed. Eng. **10,** 113–118 (1998).
19. K. Shimizu, "Optical trans-body imaging: feasibility of optical CT and functional imaging of living body," Jpn. J. of Medicina Philosophica **11,** 620–629 (1992), (in Japanese).
20. M. Kono, H. Ueki, and S. Umemura, "A new method for the identification of individuals by using of vein pattern matching of a finger," in *Proceedings of the Fifth Symposium on Pattern Measurement* (Yamaguchi, Japan, 2000), pp. 9–12, (in Japanese).
21. Y. Taki, "Non-parametric test," in Stochastic and Statistical Phenomenon II (Iwanami, Tokyo, 1973), pp. 143–148, (in Japanese).
22. R. D'Agostino and M. Stephens, "Tests based on EDF statistics," in *Goodness-of-Fit Techniques* D. B. Owen, ed. (Marcel Dekker, Inc., New York, 1986), pp. 97–193.
23. J. M. Jolion, "Table du test de Kolmogorov-Smirnov," http: rfv.insa-lyon.fr ~jolion STAT node158.html.